DOI: 10.24996/ijs.2025.66.5.26

Iraqi Journal of Science

ISSN: 0067-2904

Impact of Aerosols on the Convective Boundary Layer Development over Baghdad City

Zainab M. Abbood, Monim H. Al-Jiboori, Osama T. Al-Taai*

Department of Atmospheric Science, College of Science, Mustansiriyah University, Baghdad, Iraq.

Received: 16/10/2023 Accepted: 26/6/2024 Published: 30/5/2025

Abstract

The dynamics and physics of the atmospheric layer nearest to the Earth's surface are included in the boundary layer meteorology. This research aims to evaluate the impacts of aerosols at different altitudes with various optical properties on CBL development. The greatest impact occurs when aerosol absorption is low but close to the peak of CBL. The main objective of this research is to study the effect of aerosols which reduce the net heating, which in turn causes a decrease in the height of the CBL and increases the partitioning of the boundary layer. The methods used in the study depend on the hourly average height boundary taken from the European Centre for Weather Forecast (ECMWF) during the year 2021 over Baghdad City. It showed that the values of the height of the bounding layer during the winter were low, and they were high during the summer, while the values of the height of the bounding layer during the autumn were slightly higher than in the spring, and this was due to many reasons, such as astronomical and meteorological factors. The results showed that the values of the particulate matter $PM_{1,\ 2.5,\ \text{and}10\mu g/m3}$ during the spring and autumn were high, while the values of the $PM_{1,\ 2.5,\ \text{and}10\ \mu g/m3}$ during the winter and summer were low, as well as $PM_{10\ \mu g/m3}$ were high, including a great boundary layer height and $_{PM1,\ \text{and}\ 2.5\ \mu g/\ m3}$were low, including a slight boundary layer height. Also, PM10 µg/ m^3 was high, including a great boundary layer height and $PM_{1\ \text{and}\ 2.5}$ were low including a slight boundary layer height, and this is due to many reasons, such as the optical depth of particle matter, solar heating, humidity, wind speed, precipitation, and humans' activities.

Keywords: Baghdad; LH; ECMWF; Interaction of Aerosols; $PM_{1,\ 2.5,\ 10\ \mu g/\ m3}$.

تأثير الهباء في تطور الطبقة الحدودية الحملية فوق مدينة بغداد

زينب مجيد عبود, منعم حكيم الجبوري, أسامة طارق الطائي*

قسم علوم الجو، كلية العلوم، الجامعة المستنصرية، بغداد، العراق.

الخلاصه

تشمل الأرصاد الجوية للطبقة الحدودية على ديناميكية وفيزياء طبقة الغلاف الجوي الأقرب إلى سطح الأرض. الهدف من هذه الورقة هو تقييم تأثيرات الهباء الجوي على ارتفاعات مختلفة مع خصائص بصرية مختلفة على تطوير CBL. ان الهدف الرئيسي من البحث هو دراسة التأثير الأقوى الذي يحدث عندما يكون امتصاص الهباء الجوي منخفضًا ولكنه قريب من ذروةCBL. تعمل الأيروسولات على تقليل التسخين الصافي الذي يسبب انخفاضًا في ارتفاع CBL ويزيد من تقسيم الطبقة الحدودية. وتعتمد الطرق المستخدمة في الدراسة

*Email: osamaaltaai77@uomustansiriyah.edu.iq

على حد متوسط الارتفاع في الساعة المأخوذ من المركز الأوربي للتنبؤات الطقس (ECMWF) خلال سنة 2021 أو محطة بغداد. تبين ان ارتفاع الطبقة المحيطة خلال فصل الشتاء منخفضاً ومرتفعاً خلال فصل الصيف، بينما كانت قيم ارتفاع الطبقة المحيطة خلال فصل الخريف أعلى قليلاً مما كانت عليه في فصل الربيع، ويرجع ذلك إلى أسباب عديدة مثل العوامل الفلكيه والجويه. وأظهرت النتائج أن قيم الجسيمات (1 و2.5و10) ميكروغرام/م^3 خلال فصلي الربيع والخريف كانت مرتفعة، في حين كانت قيمها منخفضة خلال فصلي الشتاء والصيف، وكذلك كانت الجسيمات (10) ميكروغرام/ م^{3}مرتفعًا بما في ذلك ارتفاع الطبقة الحدودية وقيم الجسيمات (1 و2.5) منخفضًا بما في ذلك ارتفاع الطبقة الحدودية قليلاً. وكذلك كانPM10 ميكروغرام/ م^{3}مرتفعًا يتضمن ارتفاعًا كبيرًا للطبقة الحدية وكانPM 1و2.5 منخفضًا يتضمن ارتفاعًا طفيفًا للطبقة الحدية، ويرجع ذلك إلى العديد من الأسباب مثل العمق البصري للمادة الجسيمية والتسخين الشمسي والرطوبة وسرعة الرياح وهطول الأمطار ، بالاضافة الى نشاطات الإنسان.

1. Introduction

The boundary layer, which is the lower part of the troposphere region, is directly affected by the presence of the Earth's surface and responds to surface effects within a time scale of the order of an hour or less. These effects include surface heating, frictional clouds, heat transfer, evaporation, and the movement of local and global weather systems. The real effect of the heat that is reflected from the Earth's surface to the atmosphere over time [1] is known as the atmospheric boundary layer (ABL). The thickness of the demarcating layer changes daily and is within the range of (0.1 km) during clear and calm nights to more than (3 km) during convective days [2]. The remaining height of the troposphere above the ABL layer is called the free atmosphere (FA) (a frictionless atmosphere), as shown in Figure 1, which is defined as the height at which the effects of surface roughness disappear, the wind speed becomes equal to the geostrophic wind, and the Coriolis force becomes in equilibrium with the horizontal pressure slope force. After that, the balance of forces within the limiting layer includes the force of friction as well [3]. The boundary layer processes are primarily responsible for low clouds, such as cumulonimbus and convective transport. The boundary layer plays an important role in both the thermal and radiative balance of the atmosphere [4].

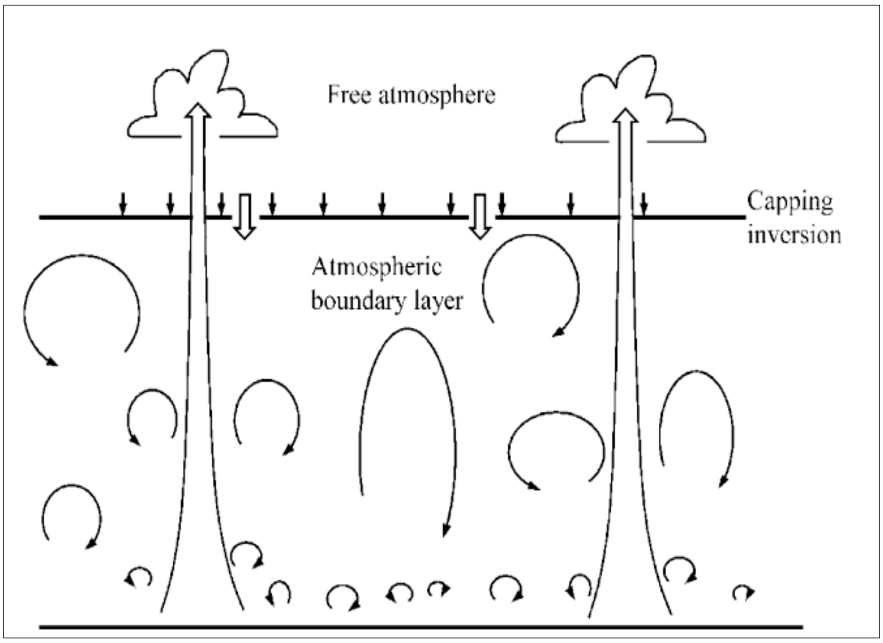

Figure 1: Division of the troposphere layer from the Earth's surface to 10 km [5].

The highest and lowest temperatures, wind shear, fog, cloud cover, and surface characteristics are all greatly influenced by the behavior of the boundary layer [6]. Wind shear, fog, and the likelihood of wind gusts are crucial considerations in wind engineering and aviation. The main components of boundary-layer meteorology include thermodynamics, radiation, surface characteristics, and turbulence. The 'viscous sublayer' is a thin laminar layer that sits just above the surface of the Earth. The equilibrium between the Earth's surface and the surface layer is adjusted by this layer [7]. A few tens of meters thick is the surface layer, also known as the inner layer. The planetary boundary layer, also known as the outer layer or Ekman layer, sits on top of the surface layer. There is a seamless transition from the surface layer to the Ekman layer. The Ekman layer's scales and those in the surface layer differ significantly [8]. Turbulent processes also have an impact on the boundary-layer dynamics in addition to average horizontal processes. Among these procedures, the most crucial one is mechanical turbulence [9]:

a) Buoyant or convective turbulence.

The importance of this research lies in the fact that the process of absorption of aerosol near the top of CBL has the strongest suppressive effect on the development of CBL near the surface or above CBL by passing the cooling effect of aerosols by attenuating incoming solar radiation and surface heat flux and the effect of the warming process by reheating the atmosphere layer with short wave radiation that absorbs and ultimately decreases the net heating rate, a matter which hinders the development of CBL and reduces the potential temperature of the mixed layer and the stability of the atmosphere.

1.1 The Structure of the Boundary Layer

The bounded layer is divided into:

a) The Earth's surface layer starts at 10% of the height of the bounded layer, and it is in the barren areas that there is a region of severe change in wind speed with height [10]. Whereas, in rural areas, it is distinguished by the stability of momentum [11].

b) The super surface layer, which is a variable layer with time during the day, it is called the convectively mixed layer in the daytime, and at night it is called the nocturnal stable layer [12]. The convective layer is an atmospheric layer located directly above the surface layer and is characterized by intense mixing resulting from heat coming from the surface of the Earth. As for the stable layer, it results when cooling occurs at the top of the surface layer, which cools the base of the mixed layer, and thus causes a decrease in buoyancy [13].

Depending on atmospheric stability and the type of dominant turbulence, ABL installations are usually classified into four types [14]:

a) Convective Boundary Layer (CBL).

b) Neutral Boundary Layer (NBL).

c) Stable (Nocturnal) Boundary Layer (SBL).

d) Cloud-Toped Boundary Layer (CTBL).

Convective Boundary Layer (CBL), in this layer, the overriding mechanism for generating turbulence in the convective boundary layer is buoyancy, as hot air masses rise because they are less dense than the surrounding air, and buoyancy is called positive buoyancy. The sources of convective currents include the transfer of heat from the hot surface of the Earth, which creates thermal cells from the warm air rising from the surface of the Earth, and the radiant cooling from the top of the cloud layer [15]. Although convective currents are dominant in the generation of turbulence, there are shear winds at the top of the mixing layer that contribute to generating turbulence in clear weather (stable weather) [16]. Turbulence acts on the intense vertical mixing of heat, moisture, and momentum in most parts of the convective boundary layer. The mixing is defined in its vertical extension by the inversion that characterizes the CBL crest.

CBL height depends on the characteristics of the area, depending on the actual temperature, mixing ratio of water vapor, pollutant concentration, and wind speed, as shown in Figures 2 and 3 [17].

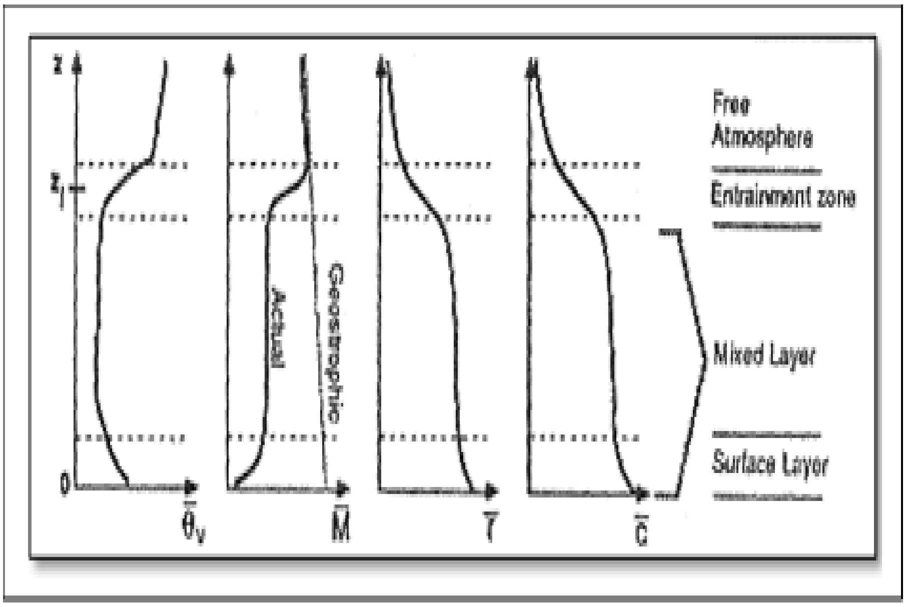

Figure 2: The average of the characteristics of the determinate layer within the convective defining layer, as (($\overline{\theta v}$) represents the actual potential temperature, ($\overline{r}$) is the mixing ratio, ($\overline{C}$) is the pollutant concentration, and ($\overline{M}$) is the wind speed [18].

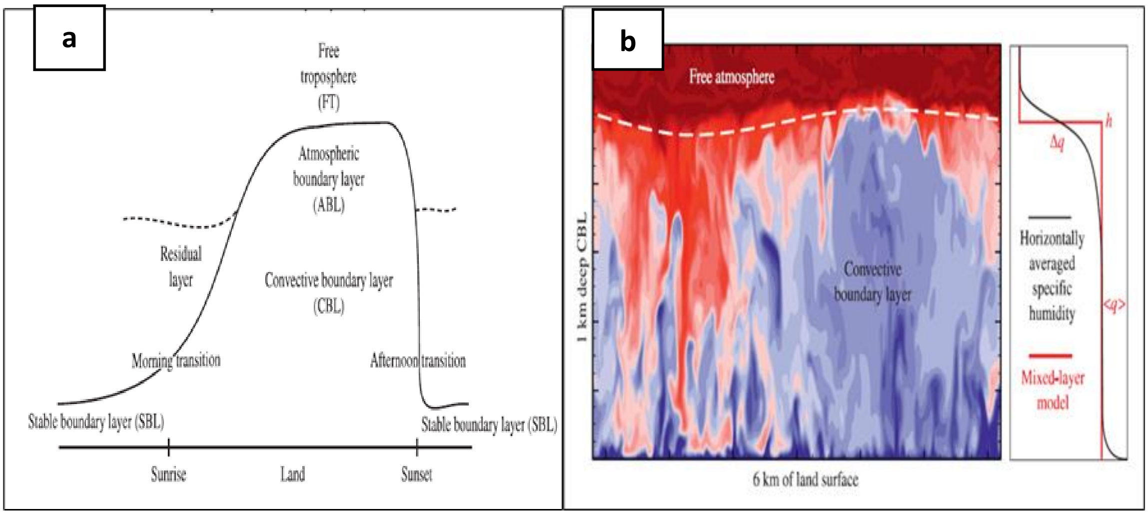

Figure 3: Schematic representation of the temporal evolution and spatial cross-section distribution of specific humidity of the atmospheric boundary layer and the relevant regions that determine its a) structure, and b) characteristics [19].

2. Materials and Methods

The work was performed using hourly data for boundary layer height and particle matter 1, 2.5, and 10 μg/m^3 taken from (ECMWF). Only one month of each season is located at its center: January (winter), April (spring), July (summer), and October (autumn) for the year 2021 over Baghdad City (this year included high concentrations of aerosols). The data was processed by MATLAB, which is a programming operation used to convert an NC file to an

Excel file and drawn by Sigma Plot. The map of Baghdad city is shown at longitude (44.25ºE) and latitude (33.25ºN) [20], as shown in Figure 4.

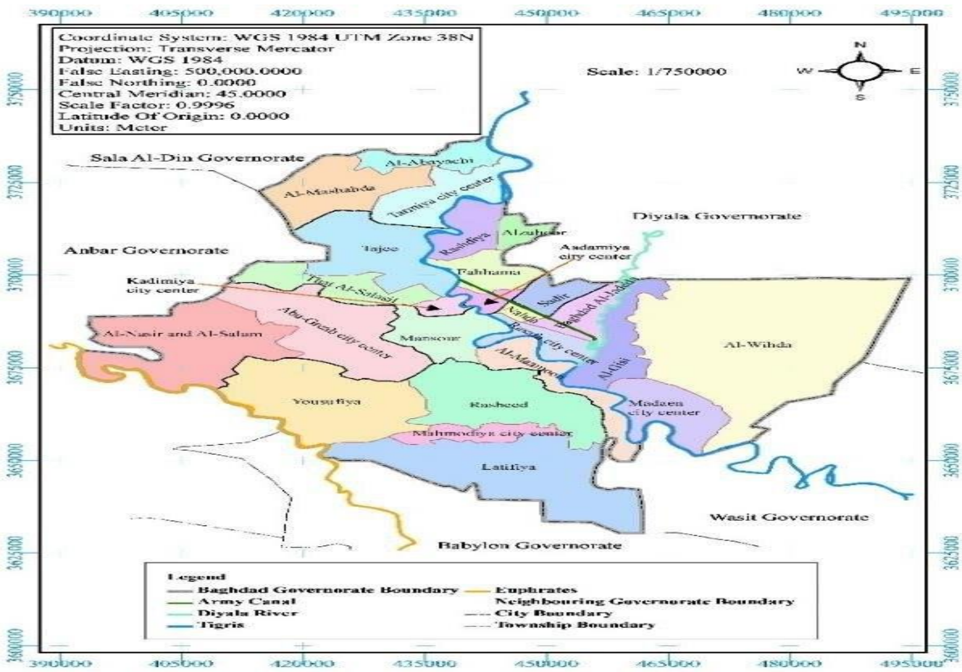

Figure 4: Baghdad map [21].

3. Results and Discussion

3.1 Analysis of the Height Behaviour of the Boundary Layer for the Baghdad City

Only one month of each season was located at its center: January (winter), April (spring), July (summer), and October (autumn) for 2021 over Baghdad city. From data analysis generally, it showed that the values of the height of the bounding layer during the winter were low, and they were high during the summer, while the values of the height of the bounding layer during the fall were slightly higher than the spring, and this is due to many reasons. During the summertime, in June 2021, the sunlight was incident vertically on the Tropic of Cancer (which is a line of latitude 3.23 degrees north of the equator), which made the heating high during the summer. When the sun rises, there is an increase in solar radiation coming to the Earth's surface, which causes the surface to heat up and leads to initiating convection. During this period, rapid growth occurs for the PBL through air entrainment above the bounding layer from above. This leads to a reduction of pollutants in the PBL, and the remaining pollutants from the previous day can be mixed into the lower layer from the surface, and this leads to an increase in the concentration of pollutants at the ground level. The height of the limiting layer reaches its greatest at midday, where it reaches (1-3) km, and then it gradually descends during the afternoon, before sunset, and the outgoing radiation flux becomes more than the downwelling flux, and this condition leads to cooling off of the surface, as it occurs more quickly at the surface than in the atmosphere and leads to the formation of an Inverted Lapse Rate (ILR), and the formation of a nocturnal boundary layer whose height is less than the convective mixing layer (about 0.1 km) as a result of suppression of turbulence with high stability, meaning that this layer changes daily due to daily cooling and heating operations. The mixing layer is shallow and superficial in the early morning hours, starting at a depth of a few tens of meters in calm weather and a few hundred meters in stormy weather. The intensity of the stable night layer, which covers the freshly formed mixing layer, causes the depth to rise gradually. The mixing layer is shallow and superficial in the early morning hours, starting at a depth of a few tens of meters in calm weather and a few hundred meters in stormy weather. The top of the mixing layer descends to the base of the residual layer (RL) many hours after daybreak as the night air warms to temperatures approaching those of the RL. The thermal masses swiftly reach the top during the second stage, causing the mixing layer's top to rise at a rate of (1) km every (15) minutes. The rate of expansion slows down as the thermal masses run into resistance when they reach the thermal inversion layer, which lies above the remaining layer (RL), and swiftly blending the layer. The mixing layer's depth remains largely consistent throughout this third stage for the majority of the afternoon. That is why the greatest disturbance intensity was during the summer season on 17/7/2021, with a value of 4904.18 as shown in Figure 5 and Table 1.

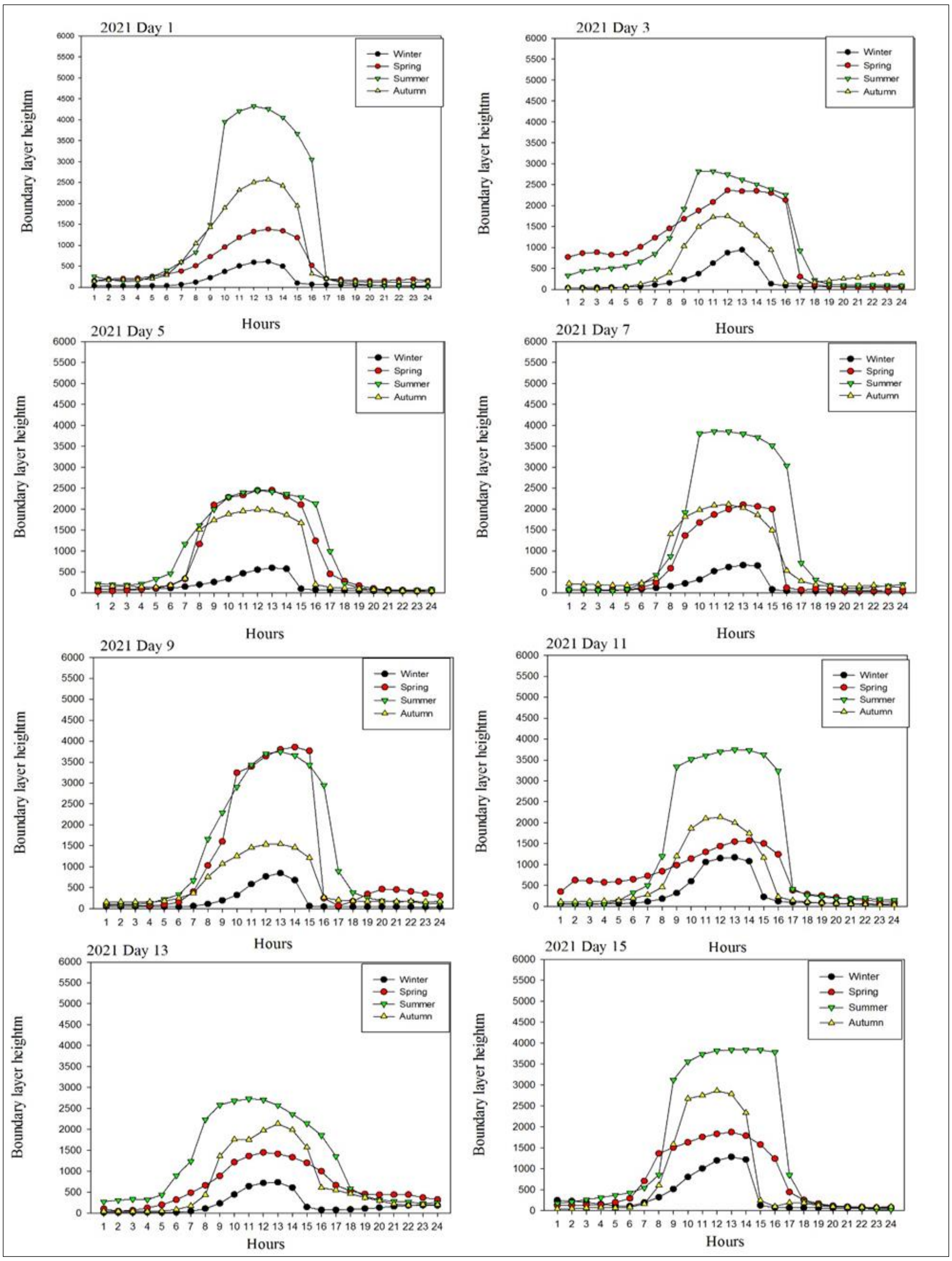

Figure 5: Height of the boundary layer over Baghdad station for the year 2021.

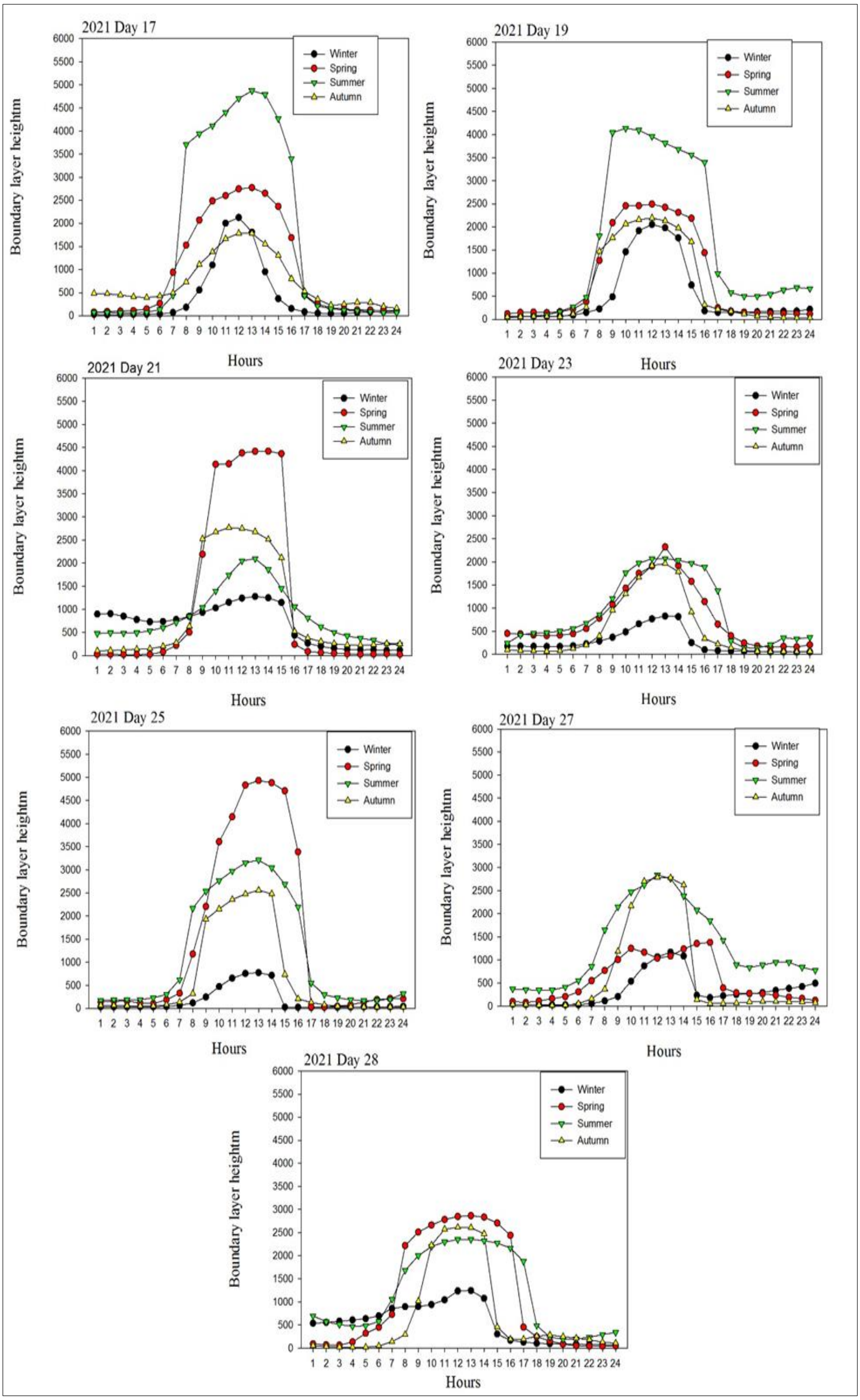

A follow up of Figure 5.

Table 1: (HS) represents the beginning of the height of the boundary layer in meters, (HP) is the greatest development, and (HE) is the end of the development of the boundary layer for the seasons (winter, spring, summer, and autumn) in Baghdad city.

Winter				
Day	**T_{am}: H_S**	**$T_{am\text{-}pm}$: H_P**	**T_{pm}: H_E**	**CTI**
1/1	06:00 60.9	12:00 607.9	22:00 23.5	584.43
1/3	05:00 65.1	12:00 943.6	20:00 60.4	883.28
1/5	05:00 107.6	13:00 569.78	22:00 30.61	539.17
1/7	06:00 112.2	12:00 656.1	22:00 22.9	633.14
1/9	06:00 58.9	12:00 843.4	17:00 39.9	803.5
1/11	06:00 113.7	12:00 1169.2	22:00 53.8	1115.36
1/13	06:00 41.1	12:00 731.6	16:00 71.7	659.93
1/15	06:00 189.7	12:00 1281.1	15:00 49.26	1231.85
1/17	06:00 67.9	11:00 2124.8	18:00 46.78	2078.02
1/19	05:00 143.0	11:00 2051.9	17:00 144.81	1907.16
1/21	06:00 774.5	10:00 1273.2	20:00 118.3	1154.85
1/23	06:00 223.3	12:00 824.3	22:00 45	779.29
1/25	06:00 63.2	12:00 771.1	16:00 19.7	751.42
1/27	06:00 52.1	12:00 1164.0	15:00 181.2	983.07
1/28	05:00 696.9	12:00 1245.8	23:00 60.3	1185.51

Spring				
Day	T_{am}: H_S	$T_{am\text{-}pm}$: H_P	T_{pm}: H_E	CTI
4/1	05:00 311.7	12:00 1383.5	19:00 153.9	1229.57
4/3	05:00 1013.2	11:00 2363.4	20:00 40.9	2322.5
4/5	05:00 172.99	12:00 2449.1	22:00 52.7	2396.43
4/7	06:00 119.7	12:00 2100.4	16:00 68.0	2032.37
4/9	06:00 399.2	12:00 3857.2	16:00 67.72	3789.51
4/11	05:00 647.6	13:00 1567.9	23:00 101.7	1466.21
4/13	05:00 317	11:00 1447.81	23:00 323.9	1123.9
4/15	05:00 287.5	12:00 1872.5	22:00 70.8	1801.69
4/17	05:00 264.9	13:00 2773.2	22:00 112.9	2660.36

4/19	05:00 216.9	11:00 2493.5	23:00 109.9	2383.52
4/21	06:00 214.4	13:00 4422.4	20:00 23.7	4398.64
4/23	06:00 554.0	12:00 2323.9	20:00 151.3	2172.58
4/25	05:00 132.0	12:00 4871.3	23:00 64.44	4806.85
4/27	05:00 309.5	15:00 1377.8	23:00 121.9	1255.86
4/28	05:00 451.8	12:00 2867.8	23:00 47.7	2820.01

A follow-up of Table 1.

Summer				
Day	**T_{am}: H_S**	**$T_{am\text{-}pm}$: H_P**	**T_{pm}: H_E**	**CTI**
7/1	05:00 396.2	12:00 4253.9	23:00 15.1	4238.79
7/3	05:00 654.0	10:00 2824.6	19:00 99.2	2725.45
7/5	05:00 461.4	11:00 2441.7	20:00 66.9	2374.8
7/7	05:00 207.0	10:00 3856.6	20:00 99.5	3757.16
7/9	05:00 336.1	12:00 3747.5	20:00 158.1	3589.38
7/11	05:00 329.5	12:00 3744.0	20:00 182.1	3561.9
7/13	05:00 892.0	10:00 2727.9	22:00 224.7	2503.19
7/15	05:00 424.7	12:00 3840.3	23:00 23.07	3817.19
7/17	05:00 182.9	12:00 4931.2	17:00 27.0	4904.18
7/19	05:00 271.7	12:00 4093.3	23:00 660.7	3432.51
7/21	05:00 599.3	10:00 2095.1	23:00 228.5	1866.67
7/23	05:00 552.2	12:00 2072.4	19:00 134.4	1938.01
7/25	06:00 617.8	12:00 3210.5	20:00 162.67	3047.83
7/27	05:00 550.8	11:00 2741	23:00 773.9	1967.11
7/28	05:00 575.8	12:00 2353.6	19:00 188.7	2164.94

Autumn				
Day	**T_{am}: H_S**	**$T_{am\text{-}pm}$: H_P**	**T_{pm}: H_E**	**CTI**
10/1	05:00 286.8	12:00 2567.5	20:00 111.38	2456.15
10/3	05:00 119.8	11:00 1745.7	16:00 122.9	1622.69
10/5	05:00 179.7	11:00 1986.9	22:00 40.23	1946.65
10/7	05:00	12:00	19:00	1964.91

	223.00	2106	141.1	
10/9	05:00 247.1	12:00 1537.9	19:00 165.45	1372.45
10/11	05:00 190.9	11:00 2128.9	23:00 33.49	2095.48
10/13	05:00 84.9	12:00 2128.8	21:00 177.9	1950.82
10/15	05:00 79.1	11:00 2858.8	15:00 95.3	2763.55
10/17	06:00 490.0	11:00 1784.6	23:00 159.8	2763.55
10/19	05:00 106.1	11:00 2189.9	22:00 25.6	2164.54
10/21	05:00 194.1	10:00 2764.8	20:00 218.8	2545.96
10/23	05:00 116.4	12:00 1961.0	20:00 51.8	1909.24
10/25	06:00 136.6	12:00 2556.7	22:00 22.9	2533.75
10/27	06:00 156.7	11:00 2782.8	16:00 53.8	2729.02
10/28	06:00 138.2	11:00 2613.6	15:00 186.9	2426.59

3.2 An analysis of the Particle Matter Behavior Includes the Boundary Layer Height for Baghdad City

Only one month of each season was located at its center: January (winter), April (spring), July (summer), and October (autumn) for the year 2021 over Baghdad city at the times 00:00 am (midday) and 12:00 pm (midnight) because there was a clear difference between night and day in aerosol concentrations, and this depended on the presence or absence of solar radiation during the day and night. Generally, throughout the year, it showed that the values of the $PM_{1,\ 2.5,\ \text{and}\ 10 \mu g/m3}$ during the spring and autumn were high, while the values of the $PM_{1,\ 2.5,\ \text{and}\ 10 \mu g/m3}$ during the winter and summer were low, as well as PM_{10} was high including a great boundary layer height, and $PM_{1 \text{and}\ 2.5}$ were low including a slight boundary layer height, as shown in Figure 6. This is due to many reasons, such as the optical depth of particle matter, solar heating, humidity, wind speed, precipitation, and humans' activities. As shown in Table 2 where PM_{10} reaches 103µg/m^3 (in spring).

Table 2: (T_S) represents the starting time, (T_P) is the greatest development, (T_E) is the end of the development of the boundary layer, and (HE) is the particle matter (1, 2.5, and 10 µg/m3) over Baghdad city.

Particle matter	Season	$T_{S\ am}$	$T_{P\ am\text{-}pm}$	$T_{E\ pm}$	PM
$PM_{1 \mu g/m}{}^3$	Winter	05:00– 06:00	11:00– 13:00	15:00–23:00	19.60
	Spring	05:00– 06:00	11:00– 13:00	16:00 –23:00	12.32
	Summer	05:00– 06:00	10:00– 12:00	19:00– 23:00	11.10
	Autumn	05:00– 06:00	10:00– 12:00	15:00–23:00	13.19
$PM_{2.5\ \mu g/m}{}^3$	Winter	05:00– 06:00	11:00– 13:00	15:00 –23:00	27.78
	Spring	05:00– 06:00	11:00– 13:00	16:00–23:00	23.98
	Summer	05:00– 06:00	10:00– 12:00	19:00– 23:00	23.24
	Autumn	05:00– 06:00	10:00– 12:00	15:00–23:00	24.41
$PM_{10\ \mu g/m}{}^3$	Winter	05:00– 06:00	11:00– 13:00	15:00 –23:00	72.17
	Spring	05:00– 06:00	11:00– 13:00	16:00 –23:00	103.17
	Summer	05:00–06:00	10:00– 12:00	19:00– 23:00	99.07
	Autumn	05:00– 06:00	10:00– 12:00	15:00–23:00	66.50

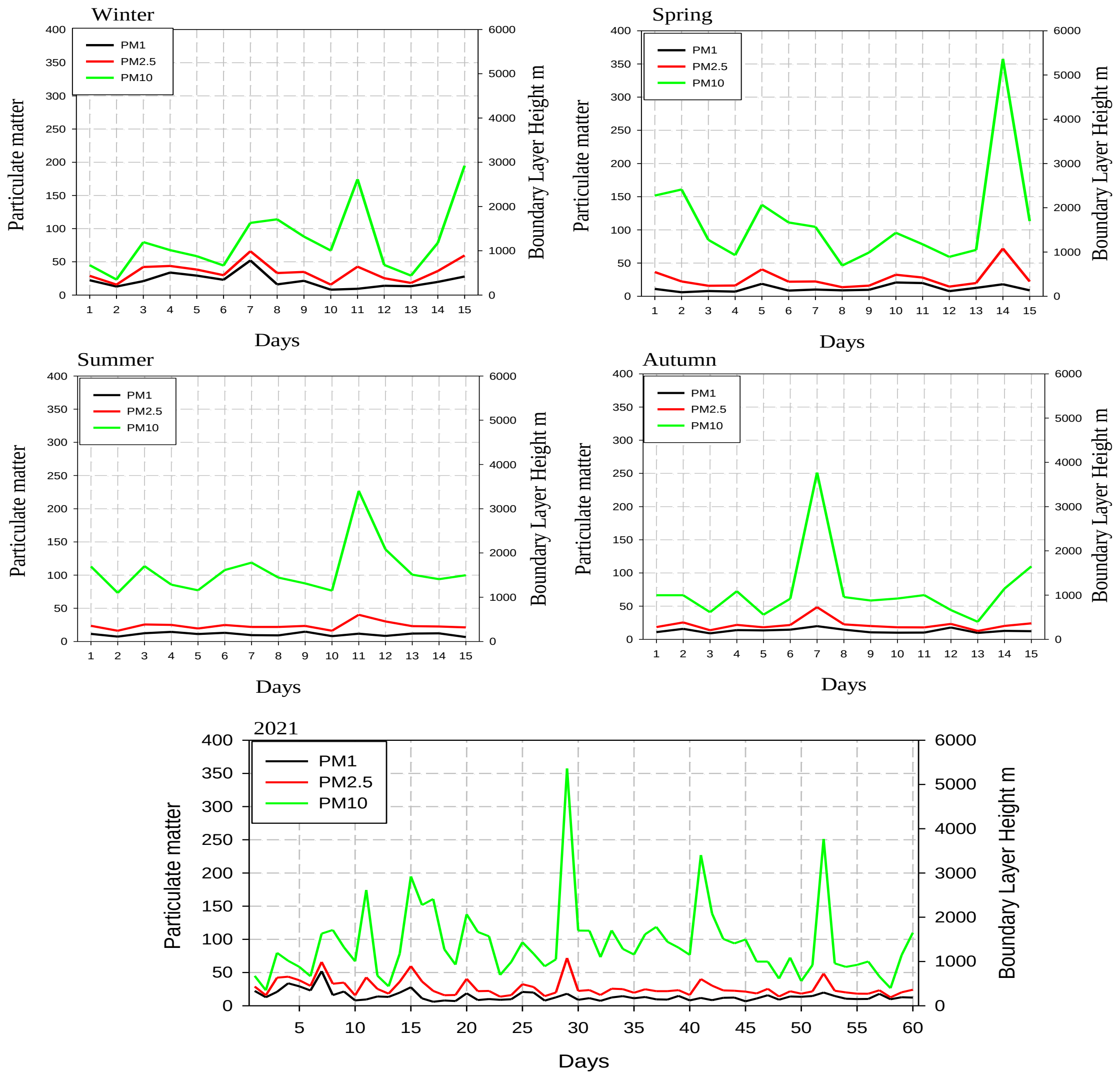

Figure 6: An analysis of the particle matter behavior, including the boundary layer height over Baghdad city for the year 2021.

4. Conclusions

From the results, we conclude that:

- The values of the height of the bounding layer during the winter were low, and they were high during the summer, while the values of the height of the bounding layer during the fall were slightly higher than in the spring, as shown in Figure 5, and this is due to many reasons, such as astronomical and meteorological factors.
- The greatest height of the bounding layer was at midday, and the lowest height was at the beginning of sunrise, and this is due to the intensity of solar radiation.
- The values of the PM during the spring and autumn were high, while the values of the PM during the winter and summer were low. Moreover, the values of PM_{10} were high including a great boundary layer height, and those of PM $_{1,\ 2.5}$ were low including a slight boundary layer height.

Acknowledgments

We would like to thank the European Center Medium Weather Forecasts (ECMWF) for the data used in this study, and we would also like to thank Mustansiriyah University for providing scientific support to accomplish this research**.**

References

[1] X. Zhang, "Aerosols consistently suppress the convective boundary layer development," *Atmospheric Research,* vol. 269, p. 106032, 2022.

[2] T. Su, "Aerosol-boundary layer interaction modulated entrainment process," *NPJ Climate and Atmospheric Science,* vol. 5, no. 1, p. 64, 2022.

[3] P. Smith, "Greenhouse gas mitigation in agriculture," *Philosophical Transactions of the Royal Society B: Biological Sciences*, vol. 363, no. 1492, pp. 789-813, 2008.

[4] F. Hourdin, "Convective boundary layer control of the sea surface temperature in the tropics," *Journal of Advances in Modeling Earth Systems,* vol. 12, no. 6, p. e2019MS001988, 2020.

[5] H. Ritchie, M. Roser, and P. Rosado, "CO_2 and greenhouse gas emissions," *Our world in data,* 2020.

[6] J. K. Casper, "Greenhouse gases: worldwide impacts," *Infobase Publishing,* 2010.

[7] K. Gillingham, and J. H. Stock, "The cost of reducing greenhouse gas emissions," *Journal of Economic Perspectives,* vol. 32, no. 4, pp. 53-72, 2018.

[8] L. A. Machado, "How weather events modify aerosol particle size distributions in the Amazon boundary layer," *Atmospheric Chemistry and Physics,* vol. 21, no. 23, pp. 18065-18086, 2021.

[9] D. Zhao, "The impact threshold of the aerosol radiation forcing on the boundary layer structure in the pollution region," *Atmospheric Chemistry and Physics Discussions,* vol. 20, no. 20, pp. 1-3, 2020.

[10] Y. Ma, "How do aerosols above the residual layer affect the planetary boundary layer height," *Science of the Total Environment,* vol. 814, p. 151953, 2022.

[11] Y. Miao, "Integrated impacts of synoptic forcing and aerosol radiative effect on boundary layer and pollution in the Beijing–Tianjin–Hebei region, China," *Atmospheric Chemistry and Physics,* vol. 20, no. 10, pp. 5899-5909, 2020.

[12] J. Li, "Aerosol radiative effects and feedbacks on boundary layer meteorology and $PM_{2.5}$ chemical components during winter haze events over the Beijing-Tianjin-Hebei region," *Atmospheric Chemistry and Physics,* vol. 20, no. 14, pp. 8659-8690, 2020.

[13] M. Kulmala, "Aerosols, clusters, greenhouse gases, trace gases and boundary-layer dynamics: On feedbacks and interactions," *Boundary-Layer Meteorology,* vol. 186, no. 3, pp. 475-503, 2023.

[14] Y. OMa, "The stove, dome, and umbrella effects of atmospheric aerosol on the development of the planetary boundary layer in hazy regions," *Geophysical Research Letters,* vol. 47, no. 13, p. e2020GL087373, 2020.

[15] Y. Yang, "Effects of aerosols on the atmospheric boundary layer temperature inversion over the Sichuan Basin, China," *Atmospheric Environment,* vol. 262, p. 118647, 2021.

[16] E. A. Rosa, and T. Dietz, "Human drivers of national greenhouse-gas emissions," *Nature Climate Change,* vol. 2, no. 8, pp. 581-586, 2012.

[17] H. M. Al-Samarrai, and M. H. Al-Jiboori, "Estimation of the Daily Maximum Air Temperature for Baghdad City Using Multiple Linear Regression," *Al-Mustansiriyah Journal of Science,* vol. 33, pp. 9-14, 2022.

[18] N. A. Mohammed, "The Relationship between Vertical Kinematic Eddy Heat Flux, Air Temperature and Turbulent Kinetic Energy in Atmospheric Boundary Layer: Baghdad City," *Al-Mustansiriyah Journal of Science,* vol. 35, no. 1, pp. 1-7, 2024.

[19] A. F. Hassoon, M. M. Ahmed, and N. M. Abd, "The Relationship between Air Stability and Visibility over Baghdad City," *Al-Mustansiriyah Journal of Science,* vol. 32, no. 2, pp. 82–89, 2021.

[20] X. Sun, Y. Zhou, T. Zhao, Y. Bai, T. Huo, L. Leng, H. He, and J. Sun, ″Effect of Vertical Wind Shear on PM2.5 Changes over Receptor Region in Central China," *Remote Sensing,* vol. 14, p. 3333, 2022.

[21] X. Zheng, ″Environmental effects on aerosol-cloud interaction in non-precipitating marine boundary layer (MBL) clouds over the eastern North Atlantic,″ *Atmospheric Chemistry and Physics, vol.* 22, no. 1, pp. 335-354, 2022.